Journal of Anesthesia & Clinical Research
ISSN: 2155-6148

Perez-Aguilar et al., J Anesth Clin Res 2012, 3:6
DOI: 10.4172/2155-6148.1000218

Research Article Open Access

Human μ Opioid Receptor Models with Evaluation of the Accuracy Using the Crystal Structure of the Murine μ Opioid Receptor

Jose Manuel Perez-Aguilar[1], Jeffery G. Saven[1]* and Renyu Liu[2]*

[1]*Department of Chemistry, University of Pennsylvania, Philadelphia, 19104, USA*
[2]*Department of Anesthesiology and Critical Care, Hospital of University of Pennsylvania, Philadelphia, 19104, USA*

Abstract

Models of the human μ opioid receptor were constructed using available G-protein-coupled receptor (GPCR) structures using homology (comparative) modeling techniques. The recent publication of a high-resolution crystal structure of a construct based on the murine μ opioid receptor offers a unique opportunity to evaluate the reliability of the homology models and test the relevance of introducing more templates (known structures) to increase the accuracy of the comparative models. In the first model two templates were used: the β_2 adrenergic and bovine rhodopsin receptors. For the second model, four templates were utilized: the β_2 adrenergic, bovine rhodopsin, β_1 adrenergic, and A_{2A} adenosine receptors. Including additional templates improved the accuracy of structural motifs and other features of the model when the same sequence alignment was used. The predicted structures were especially relevant in the case of important receptor regions such as the DRY motif, which has been associated with receptor activation. Additionally, this study showed that receptor sequence similarity is crucial in homology modeling, as indicated in the case of the highly diverse EC2 loop. This study demonstrates the reliability of the homology modeling technique in the case of the μ opioid receptor, a member of the rhodopsin-like family class of GPCRs. The addition of more templates improved the accuracy of the model. The findings regarding the modeling has significant implication to other GPCRs where the crystal structure is still unknown and suggest that homology modeling techniques can provide high quality structural models for interpreting experimental findings and formulating structurally based hypotheses regarding the activity of these important receptors.

Keywords: Human μ opioid receptor; Murine μ opioid receptor; G-protein-coupled receptor (GPCR); Homology modeling

Introduction

Opioid receptors are part of the largest family of integral transmembrane proteins coded by the human genome, the G-protein-coupled receptors (GPCRs) [1]. GPCRs mediate most transmembrane signal transduction, usually in response to hormones, neurotransmitters and environmental stimulants. Each GPCR comprises an extracellular N terminus, seven-transmembrane (7TM) helical segments separated by alternating intracellular and extracellular loop regions, and an intracellular C terminus [1-3]. Opioid receptors are part of the largest family of GPCRs, family A or rhodopsin-like GPCRs [4]. Other family A members include the receptors for epinephrine, dopamine, serotonin, and adenosine [5]. The μ opioid receptor is the primary receptor in the brain for endogenous opioid neuropeptides as well as exogenously administrated opioid compounds [6-8]. Potent drugs such as morphine, heroin, fentanyl and methadone induce their pharmacological effects through the activation of this receptor [9].

Extensive computational comparative modeling of the μ opioid receptor was used to suggest structural details of this important signal transduction protein [10-15] before the crystal structure of the murine μ opioid receptor was revealed [16]. The μ opioid receptor has been heavily modeled using the few receptor structures available at the time due to its importance related to addiction and pain control and reward pathways [6,7,12,14]. More recently, the addition of several GPCR structures in recent years opens the potential opportunity for higher quality modeled structures. Within the past few years, our group has constructed different versions of homology models of human μ opioid receptor (hMOP-R) based on the available structural information at that time. The recent publication of a high-resolution crystal structure of murine μ opioid receptor solution offers a unique opportunity to evaluate the reliability of the modeling of GPCRs of this family using other GPCR structures and to test the relevance of introducing more templates to increase the accuracy of the comparative models.

Methods

Two different homology models were constructed in our group before the crystal structure of murine μ opioid receptor was disclosed: (i) The first model, named as 2T-hMOP-R, used the X-ray crystallographic structures of human β_2 adrenergic receptor at 2.4 Å resolution (PDB accession code: 2RH1) [17] and bovine rhodopsin at 2.2 Å resolution (PDB accession code: 1U19) [18] as templates. (ii) the second model, named as 4T-hMOP-R, used the X-ray crystallographic structures of turkey β_1 adrenergic receptor at 2.7 Å resolution (PDB accession code: 2VT4) [19] and human A2A adenosine receptor at 2.6 Å resolution (PDB accession code: 3EML) [20] in addition to the above mentioned 2 templates.

Given the importance of sequence alignments in the comparative modeling procedure [21-23], several different programs and substitution matrices were considered. The sequences of hMOP-R, human β_2 adrenergic receptor, bovine rhodopsin, turkey β_1 adrenergic receptor and human A_{2A} adenosine receptor were obtained from the UniProt Knowledgebase UniProtKB server with the accession numbers

***Corresponding authors:** Jeffery G. Saven, Department of Chemistry, University of Pennsylvania, 231 South 34th Street, Philadelphia, PA 19104 USA, Tel: 215-573-6062; Fax: 215-573-6416; E-mail: saven@sas.upenn.edu

Renyu Liu, MD, Ph.D, Assistant Professor, Department of Anesthesiology and Critical Care, Perelman School of Medicine at the University of Pennsylvania, 336 John Morgan building,3620 Hamilton Walk, Philadelphia, PA 19104; Tel: 2156623750; Fax: 2153495078; E-mail: liur@uphs.upenn.edu

Received June 25, 2012; **Accepted** June 30, 2012; **Published** June 02, 2012

Citation: Perez-Aguilar JM, Saven JG, Liu R (2012) Human μ Opioid Receptor Models with Evaluation of the Accuracy Using the Crystal Structure of the Murine μ Opioid Receptor. J Anesth Clin Res 3:218. doi:10.4172/2155-6148.1000218

Copyright: © 2012 Perez-Aguilar JM, et al. This is an open-access article distributed under the terms of the Creative Commons Attribution License, which permits unrestricted use, distribution, and reproduction in any medium, provided the original author and source are credited.

P35372, P07550, P02699, P07700, and P29274, respectively [24]. *BLASTp* [25], *SIM* [26], *ClustalW* [27], and *Phyre* [28] were used to align the sequences of hMOP-R and human β_2 adrenergic receptor. In the case of *BLASTp*, three members of the "Blosum" substitution matrix family [29] (Blosum62, Blosum45 and Blosum80) and one member of the "PAM" substitution matrix family [30] (PAM70) were used. For the case of the alignment tool SIM, Blosum62 and Blosum30 were used. For *ClustalW* just the Blosum30 matrix was used. The protein structure prediction server *Phyre*, was also utilized. Standard penalty gaps were applied in all the cases [25-27]. A similar procedure was carried out in the case of hMOP-R and bovine rhodopsin, hMOP-R and β_1 adrenergic receptor, and hMOP-R and A_{2A} adenosine receptor.

A final sequence alignment was obtained for each pair of proteins and modifications were performed to maintain highly conserved fingerprint residues of the rhodopsin-like GPCR family [31]. Among these are: the *disulfide bond* between TM3 and the second extracellular loop (EC2), the "DRY" motif in TM3, the *XBBXXB* motif in the third intracellular loop (IC3) (where B represents a basic amino acid and X represents a non-basic residue, LRRITR in the case of hMOP-R), the *FXXXWXPX*[*F*] motif in TM6 (*FIVCWTPIH* in the case of hMOP-R), the *NPXXY* motif in TM7 (*NPVLY* in hMOP-R), and the C-terminal cys palmitoylation site [31]. The final multiple sequence alignment is presented in figure 1.

Using the sequence alignments and the two- and four-template structure sets described above, one hundred models of the human μ opioid receptor models (from residue 65 to 353) in each case were generated using Modeller 9v2 with the refinement optimization level adjusted to *slow* [32,33]. The side chains from the resulting models of the four-template and two-template ensembles, were minimized using NAMD2 [34] and the CHARMM22 force field [35]. Hydrogen atoms were added and minimization was performed by the conjugate-gradient method until the total energy remains constant (change in energy less than 1.0 kcal/mol). Models with the lowest energy were selected and characterized using Molprobity [36] to confirm that no steric clashes or unusual conformations of the backbone and side chains were present. Herein, the selected structures from the four- and two-template sets are denominated 4T-hMOP-R and 2T-hMOP-R, respectively. The secondary structures of the models were assigned with STRIDE [37], and the locations and lengths of the TM helices were the same for both 4T-hMOP-R and 2T-hMOP-R. The X-ray crystallographic structure murine μ opioid receptor (PDB accession code: 4DKL) was used to evaluate these models. Renderings of molecular structures for comparison were generated using PyMOL (http://www.pymol.org/, Version 1.3, Schrödinger, LLC).

Results and Discussion

Comparison between models 4T-hMOP-R and 2T-hMOP-R

Two different views of the model of hMOP-R are depicted in Figure 2a. In general, 4T-hMOP-R and 2T-hMOP-R are similar with a backbone rmsd of 1.30 Å. One of the most significant differences between the models is a helical segment in IC2 that is specific to the β_1 adrenergic receptor and A_{2A} adenosine receptor; it is absent in 2T-hMOP-R (see inset of Figure 2a). This loop connects helices TM3 and TM4 and is close to the important and highly conserved *DRY*

Figure 1: Sequence alignment used in the creation of the models of the human μ opioid receptor, hMOP-R. The templates are: human β_2 adrenergic receptor (ADRβ_2), bovine rhodopsin (bRHO), turkey β_1 adrenergic receptor (ADRβ_1) and human A_{2A} adenosine receptor (AA2AR). The residues of the N- and C- terminus are excluded (residue 1 to 65 and residues 354 to 400, respectively). Also, the residues excluded from the comparative modeling are colored in gray. The most conserved residues at each of the transmembrane helices are depicted in blue. The secondary structure of the β_2 adrenergic receptor based on STRIDE [32], is shown below the sequences. Residue numbering of hMOP-R is shown. Highly conserved motifs in the rhodopsin-like GPCR family are highlighted in yellow.

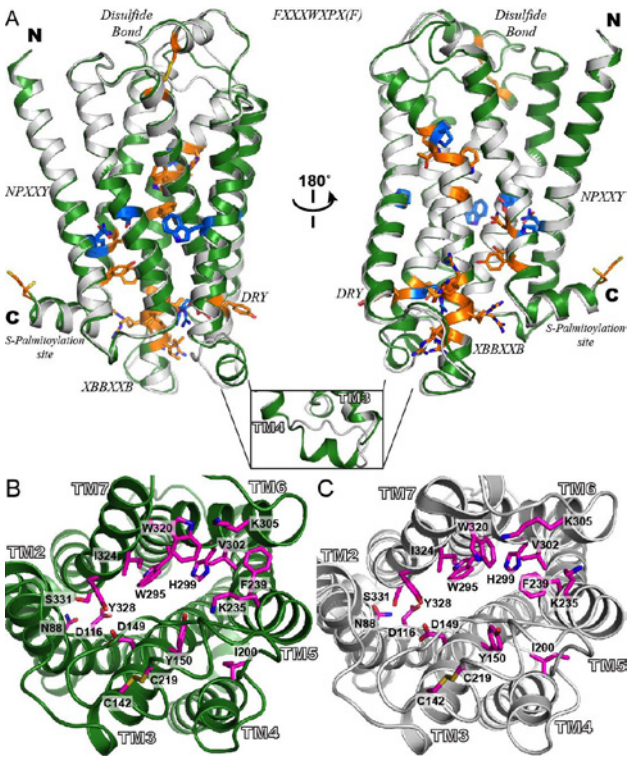

Figure 2: Alignment and comparison of representative models of hMOP-R. (A) the representative models from the four-template ensemble (4T-hMOP-R) and two-template ensemble (2T-hMOP-R) are color in green and white, respectively. The most conserved residues at each of the transmembrane helices are depicted as blue sticks. The highly conserved motifs in the rhodopsin-like GPCR family are depicted as orange sticks; disulfide bond between TM3 and EC2, DRY in TM3, XBBXXB in IC3 (where B represents a basic amino acid and X represents a non-basic residue), FXXXWXPX[F] in TM6, the NPXXY in TM7 and the C-terminal cys palmitoylation site. The inset at the bottom shows one of the most significant differences between the two models. The IC2 loop that connects helices TM3 and TM4 in the 4T-hMOP-R model, forms a helical motif inherit from the β1 adrenergic receptor and the A2A adenosine receptor templates. (B) Top views of the binding site for the 4T-hMOP-R and 2T-hMOP-R models with a set of the relevant residues involved in ligand interaction based on mutagenesis studies. Side chain residues are colored in magenta in both cases. This view of the hMOP-R from the extracellular side of the membrane shows the counterclockwise arrangement of the TM helices.

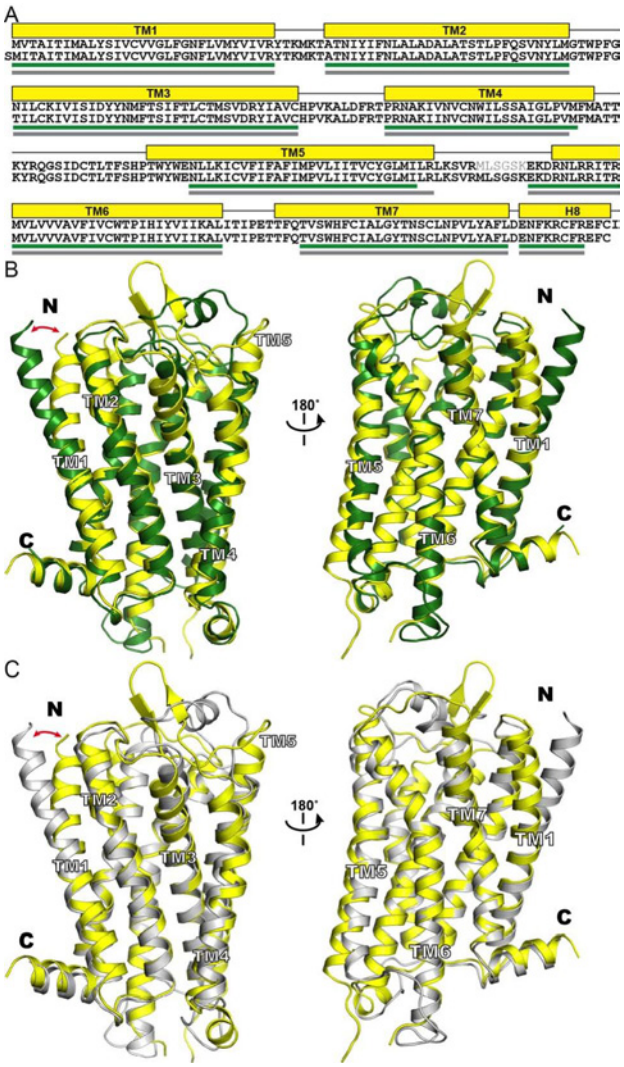

Figure 3: Comparison of the structure of mouse μ opioid receptor with the models of the human μ opioid receptor 4T-hMOP-R and 2T-hMOP-R. (A) Sequence alignment that displays the length of the TM helices in the crystal structure (top sequence) and the 4T-hMOP-R and 2T-hMOP-R models (bottom sequence). The helical segments are depicted as yellow boxes for the crystal structure and as green and gray lines for 4T-hMOP-R and 2T-hMOP-R, respectively. (B) Crystal structure (yellow) and the 4T-hMOP-R model (green) are superimposed. (C) Crystal structure (yellow) and the 2T-hMOP-R model (gray) are superimposed. The red arrow indicates the different position of the extracellular half of the TM1 helix.

motif. In general, both structures could be used to interpret different experimental studies associated with ligand binding properties of the μ opioid receptor (see Figure 2b).

Comparison of the constructed models with the crystal structure of mouse μ opioid receptor

The human (uniprot accession number P35372) and mouse (uniprot accession number P42866) μ opioid receptors has a sequence identity of 94% if the entire receptor sequences are considered and a sequence identity of 99% for the structure solved in the crystal structure. The sequence identity between human and mouse μ opioid receptor suggests that both proteins likely share a very similar structure.

The representative models from the comparative modeling procedure were compared with the crystal structure of murine μ opioid receptor (PDB accession code: 4DKL). The root-mean-square deviation (rmsd) of the Cα atoms located in the TM helices (Figure 3A) between the crystal structure and 4T-hMOP-R and 2T-hMOP-R is 2.67 Å and 2.60 Å, respectively. Superposition of the structures is shown in figure 3. As seen from the rmsd values, both modeled structures are, in general, very similar to the crystal structure. Interestingly, one of the main differences comes from the extracellular portion of TM1. In the crystal structure, this segment of TM1 presents a position that is closer (~ 10 Å) to the rest of the helical bundle (Figure 3B and 3C). This relative position is not seen in any of the templates and thus, not present in the models. Interestingly and despite the sequence identity, the recent structure of a closely related receptor, the human κ opioid receptor [16] presents the same segment of TM1 with an outward displacement similar to the templates (and the models) presented here. This displacement has been suggested to reflect difference in crystallization conditions or crystal packing [19-38].

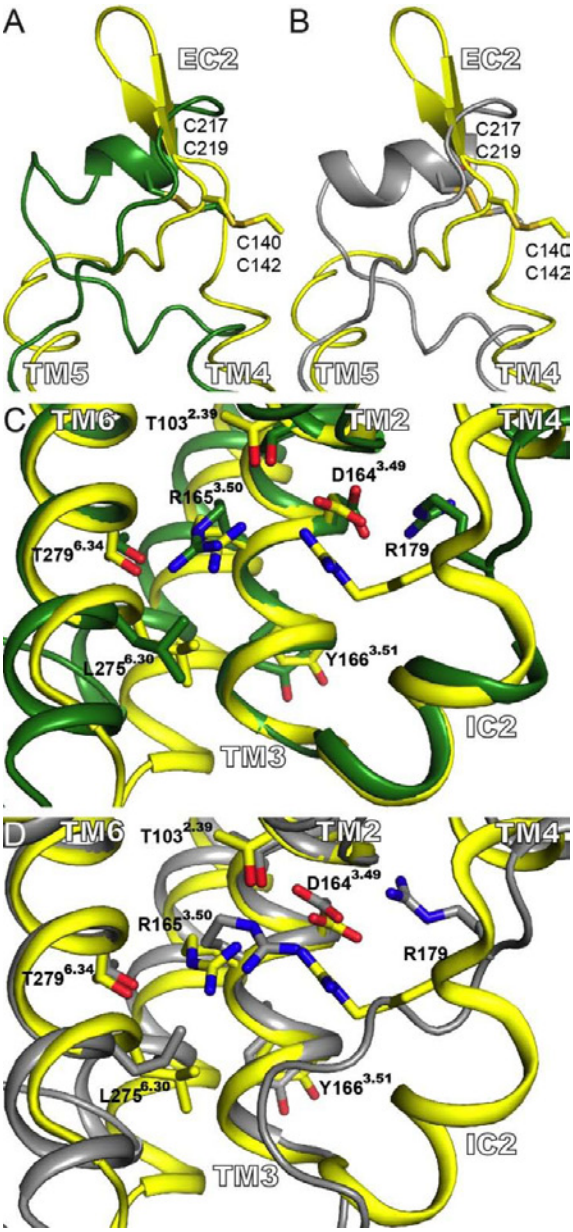

Figure 4: Structure of the EC2 and IC2. (A) and (B) Superposition of the EC2 for the crystal structure (yellow) and the 4T-hMOP-R (green) and 2T-hMOP-R (gray) models, respectively. The conserved disulfide bond between C140 in TM3 and C217 in EC2 is displayed. The numbers below correspond to the residue number for the equivalent residues in the human μ opioid receptor (C219 and C142). (C) and (D) display views from the intracellular milieu, particularly interactions around the DRY motif. In (C) a comparison of the crystal structure (yellow) with 4T-hMOP-R (green) is shown. In (D) comparison of the crystal structure (yellow) with 2T-hMOP-R (gray) is shown. Relevant side chains are depicted.

The extracellular loop (EC2)

An interesting case is the structure adopted by the second extracellular loop (EC2) that, when compared with TM region, presents a larger sequence diversity among the μ receptor and the template proteins. In the models the structure of EC2 was modeled mainly using the information from the β_2 adrenergic receptor in 2T-hMOP-R and β_2 and β_1 adrenergic receptors in 4T-hMOP-R. In both cases, EC2 forms a short helix, partially inherited from the adrenergic receptors. In the crystal structure of murine μ opioid receptor the EC2 loop forms a β-sheet structure. Interestingly, the positions of the cysteine residues that form the highly conserved disulfide bond were predicted correctly in both models figure 4A and 4B.

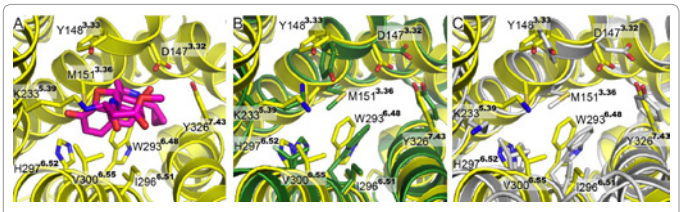

Figure 5: Binding pocket comparison. (A) The binding pocket of the crystal structure of mouse μ opioid receptor with the structure of β-FNA (magenta) is displayed. The nine residues that directly interact with β-FNA are indicated. (B) and (C) Comparison of the nine residues in the binding pocket of the crystal structure (yellow) and the 4T-hMOP-R (green) and 2T-hMOP-R (gray) models, respectively.

The conserved DRY motif

Another important feature is the set of interactions around the conserved DRY motif (Figure 4C and 4D). In bovine rhodopsin, the highly conserved residue $R135^{3.50}$ is forming a salt-bridge with E247$^{6.30}$. This interaction, sometimes denominated "ionic lock", is not present in the crystal structure of the μ opioid receptor (also this interaction is not seen in the other three templates utilized in this study). In the case of the crystal structure of the μ opioid receptor, the equivalent position, $R165^{3.50}$, is interacting with the side chain of $T279^{6.34}$. This polar interaction is correctly predicted in both, 4T-hMOP-R and 2T-hMOP-R structures, (Figures 4C and 4D). In general terms, most of the residues around the DRY motif, as well as the interactions, are properly predicted in both representative models. The exception is the conformation of the long side chain of residue R179 located in the IC2 loop. The helical structure of this loop in 4T-hMOP-R is in good agreement with the structure seeing in the crystal structure, figure 4C. Because neither bovine rhodopsin nor the β_2 adrenergic receptor presents helical content in this loop, the structure of IC2 in 2T-hMOP-R does not reproduce correctly the topology seen in the crystal structure. Despite the correct prediction of the helical content of IC2 in 4T-hMOP-R, the conformation of the long side chain of R179 is not properly modeled, even though the interaction of R179 with $D164^{3.49}$ is correctly predicted in both 4T-hMOP-R 2T-hMOP-R and (Figure 4D).

The binding pocket

The analysis of the binding pocket in the crystal structure of the μ opioid receptor shows important features that are conserved in the model structures. Both, 4T-hMOP-R and 2T-hMOP-R correctly orient the side chain of $K233^{5.39}$ toward the binding pocket where it could covalently bind β-FNA, as observed in the crystal structure. The nine positions that directly interact with β-FNA in the crystal structure ($D147^{3.32}$, $Y148^{3.33}$, $M151^{3.36}$, $K233^{5.39}$, $W293^{6.48}$, $I296^{6.51}$, $H297^{6.52}$, $V300^{6.55}$, and $Y326^{7.43}$) are displayed in figure 5A. These residues from the crystal structure are compared with the equivalent residues in 4T-hMOP-R and 2T-hMOP-R (Figures 5B and C). In general, the orientation of the side chains of these nine residues was correctly modeled with rmsd values with the side chains atom of the crystal structure of 1.4 Å and 1.6 Å for the 4T-hMOP-R and 2T-hMOP-R, respectively, even though no ligand was present in creating the models.

In conclusion, using the newly available crystal structure the murine μ opioid receptor, we demonstrated the relative accuracy of

the homology modeling for μ opioid receptor. The addition of more templates improved the accuracy of the model. This was especially relevant in the case of important receptor regions such as the DRY motif, which has been related with receptor activation, and the ligand binding pocket. Additionally, this study shows that some degree of receptor sequence similarity is useful in homology modeling: in the case of the loop EC2 where little consensus in about the alignment was observed, a β-sheet rather than α-helical structure was observed in the crystal structure. The findings have significant implication for the construction of model structures of GPCRs, particularly those of the same family, where crystal structures are still unavailable. Such models can guide the interpretation of experimental findings, the creation of structure-based models for receptor activation, and the formulation of hypotheses regarding these important receptors.

References

1. Rosenbaum DM, Rasmussen SG, Kobilka BK (2009) The structure and function of G-protein-coupled receptors. Nature 459: 356-363.
2. Pierce KL, Premont RT, Lefkowitz RJ (2002) Seven-transmembrane receptors. Nat Rev Mol Cell Biol 3: 639-650.
3. Hanson MA, Stevens RC (2009) Discovery of new GPCR biology: one receptor structure at a time. Structure 17: 8-14.
4. Fredriksson R, Lagerstrom MC, Lundin LG, Schioth HB (2003) The G-protein-coupled receptors in the human genome form five main families. Phylogenetic analysis, paralogon groups, and fingerprints. Mol Pharmacol 63:1256-1272.
5. Lagerstrom MC, Schioth HB (2008) Structural diversity of G protein-coupled receptors and significance for drug discovery. Nat Rev Drug Discov 7: 339-357.
6. Kieffer BL, Evans CJ (2009) Opioid receptors: From binding sites to visible molecules in vivo. Neuropharmacology 56: 205-212.
7. Waldhoer M, Bartlett SE, Whistler JL (2004) Opioid receptors. Annu Rev Biochem 73: 953-990.
8. Moles A, Kieffer BL, D'Amato FR (2004) Deficit in attachment behavior in mice lacking the mu-opioid receptor gene. Science 304: 1983-1986.
9. Contet C, Kieffer BL, Befort K (2004) Mu opioid receptor: a gateway to drug addiction. Curr Opin Neurobiol 14: 370-378.
10. Filizola M, Carteni-Farina M, Perez JJ (1999) Molecular modeling study of the differential ligand-receptor interaction at the mu, delta and kappa opioid receptors. J Comput Aided Mol Des 13: 397-407.
11. Subramanian G, Paterlini MG, Portoghese PS, Ferguson DM (2000) Molecular docking reveals a novel binding site model for fentanyl at the mu-opioid receptor. J Med Chem 43: 381-391.
12. Zhorov BS, Ananthanarayanan VS (2000) Homology models of mu-opioid receptor with organic and inorganic cations at conserved aspartates in the second and third transmembrane domains. Arch Biochem Biophys 375: 31-49.
13. Fowler CB, Pogozheva ID, LeVine H, Mosberg HI (2004) Refinement of a homology model of the mu-opioid receptor using distance constraints from intrinsic and engineered zinc-binding sites. Biochemistry 43: 8700-8710.
14. Zhang Y, Sham YY, Rajamani R, Gao J, Portoghese PS (2005) Homology modeling and molecular dynamics simulations of the mu opioid receptor in a membrane-aqueous system. Chembiochem 6: 853-859.
15. Bera I, Laskar A, Ghoshal N (2011) Exploring the structure of opioid receptors with homology modeling based on single and multiple templates and subsequent docking: A comparative study. J Mol Model 17: 1207-1221
16. Wu H, Wacker D, Mileni M, Katritch V, Han GW, et al. (2012) Structure of the human k-opioid receptor in complex with JDTic. Nature 485: 327-332.
17. Cherezov V, Rosenbaum DM, Hanson MA, Rasmussen SG, Thian FS, et al. (2007) High-resolution crystal structure of an engineered human beta2-adrenergic G protein-coupled receptor. Science 318: 1258-1265.
18. Okada T, Sugihara M, Bondar AN, Elstner M, Entel P, et al. (2004) The retinal conformation and its environment in rhodopsin in light of a new 2.2 A crystal structure. J Mol Biol 342: 571-383.
19. Warne T, Serrano-Vega MJ, Baker JG, Moukhametzianov R, Edwards PC, et al. (2008) Structure of a beta1-adrenergic G-protein-coupled receptor. Nature 454: 486-491.
20. Jaakola VP, Griffith MT, Hanson MA, Cherezov V, Chien EY, et al. (2008) The 2.6 angstrom crystal structure of a human A2A adenosine receptor bound to an antagonist. Science 322: 1211-1217.
21. Baker D, Sali A (2001) Protein structure prediction and structural genomics. Science 294: 93-96.
22. Michino M, Abola E, Brooks CL, Dixon JS, Moult J, et al. (2009) Community-wide assessment of GPCR structure modelling and ligand docking: GPCR Dock 2008. Nat Rev Drug Discov 8: 455-463.
23. Marti-Renom MA, Stuart AC, Fiser A, Sanchez R, Melo F, et al. (2000) Comparative protein structure modeling of genes and genomes. Annu Rev Biophys Biomol Struct 29: 291-325.
24. Jain E, Bairoch A, Duvaud S, Phan I, Redaschi N (2009) Infrastructure for the life sciences: design and implementation of the UniProt website. BMC Bioinformatics 10: 136.
25. Altschul SF, Gish W, Miller W, Myers EW, Lipman DJ (1990) Basic local alignment search tool. J Mol Biol 215: 403-410.
26. Gasteiger E, Gattiker A, Hoogland C, Ivanyi I, Appel RD, et al. (2003) ExPASy: The proteomics server for in-depth protein knowledge and analysis. Nucleic Acids Res 31: 3784-3788.
27. Larkin MA, Blackshields G, Brown NP, Chenna R, McGettigan PA et al. (2007) Clustal W and Clustal X version 2.0. Bioinformatics 23: 2947-2948.
28. Kelley LA, Sternberg MJ (2009) Protein structure prediction on the Web: a case study using the Phyre server. Nat Protoc 4: 363-371.
29. Henikoff S, Henikoff JG (1992) Amino acid substitution matrices from protein blocks. Proc Natl Acad Sci U S A 89: 10915-10919.
30. Schwartz RM, Dayhoff MO (1978) Improved scoring matrix for identifying evolutionary relatedness among proteins. Biophys J 21: A198.
31. Surratt CK, Adams WR (2005) G protein-coupled receptor structural motifs: relevance to the opioid receptors. Curr Top Med Chem 5: 315-324.
32. Sali A, Blundell TL (1993) Comparative protein modelling by satisfaction of spatial restraints. J Mol Biol 234: 779-815.
33. Eswar N, Webb B, Marti-Renom MA, Madhusudhan MS, Eramian D, et al. (2006) Comparative protein structure modeling using Modeller. Curr Protoc Bioinformatics Chapter 5:Unit 5.6.
34. Phillips JC, Braun R, Wang W, Gumbart J, Tajkhorshid E, et al. (2005) Scalable molecular dynamics with NAMD. J Comput Chem 26: 1781-1802.
35. MacKerell AD, Bashford D, Bellott M, Dunbrack RL, Evanseck JD, et al. (1998) All-atom empirical potential for molecular modeling and dynamics studies of proteins. Journal of Physical Chemistry B 102: 3586-3616.
36. Chen VB, Arendall WB, Headd JJ, Keedy DA, Immormino RM, et al. (2010) MolProbity: all-atom structure validation for macromolecular crystallography. Acta Crystallogr D Biol Crystallogr 66: 12-21.
37. Frishman D, Argos P (1995) Knowledge-based protein secondary structure assignment. Proteins 23: 566-579.
38. Granier S, Manglik A, Kruse AC, Kobilka TS, Thian FS, et al. (2012) Structure of the delta-opioid receptor bound to naltrindole. Nature 485: 400-404.